RSC Advances

ROYAL SOCIETY OF CHEMISTRY

www.rsc.org/advances

Boric acid assisted formation of mesostructure silica: from hollow spheres to hierarchical assembly

Jianping Yang,[a, b,] * Wangyuan Chen,[a] Xianqiang Ran,[a] Wei Wang,[a] Jianwei Fan, [a] and Wei-xian Zhang [a]

[a] College of Environmental Science and Engineering, State Key Laboratory of Pollution Control and Resources Reuse, Tongji University, Shanghai 200092, P. R. China

[b] Department of Chemistry, Laboratory of Advanced Materials, Fudan University, Shanghai 200433, P. R. China

E-mail: zcjpyang@gmail.com

Tel: 86-21-65985885

Abstract

A boric acid assisted assembly approach has been provided to prepare the mesostructure silica with various morphologies and porosities. The hollow siliceous spheres with ultrasmall size (~ 15 nm) can be synthesized under such ultra-dilute CTAB/P123 surfactant concentration, with TEOS as the silica source in weak acid system. It also found the ratio of CTAB/P123, the concentration of boric acid and surfactant, the amount of TEOS and the addition of $MgSO_4$ acted key roles to control the morphologies and porosity. The obtained mesostructure silica possess ordered structure, uniform morphologies (hollow sphere, tubular and cage-like mesoporous silica), high surface area (304.2 – 742.0 m^2g^{-1}), tunable large pore volume (0.55 – 2.07 cm^3g^{-1}) and pore size distribution (2.2 – 11.8 nm).

Keywords: mesoporous silica, boric acid, co-surfactant, self-assembly, hollow siliceous sphere.

1. Introduction

In recent years, mesoporous nanomaterials have received increasing attention because of their specific physical and chemical properties, such as large surface area, tunable pore size, easy functionalization, various compositions and frameworks, and thus many breakthrough applications in catalysis, adsorption, electrochemistry and biology.[1-7] As an important mesoporous nanomaterial with numerous practical applications, silica has attracted significant interesting since its designable porosity and excellent biocompatibility.[8] Current methodologies to produce the mesoporous silica nanomaterials are based on the cooperative self-assembly between surfactant and silicates precursor, with controllable nanoscale architecture, unique morphologies and frameworks.[9-12] For example, mesoporous silica nanoparticles (MSN) have become highly promising as the carrier to delivery drugs into cancer cell and realize controllable release for bioapplications.[8, 13-16] A frequently used approach to synthesize MSN is a surfactant-assistant sol-gel process by using hexadecyltrimethylammonium (CTA^+) cationic surfactant as template in the alkaline solution.[17-20] As another typical mesoporous silica material, SBA-15 has been prepared with the triblock copolymer Pluronic P123 (PEO_{20}-PPO_{70}-PEO_{20}) as the template under strong acidic conditions.[21] This simple self-assembly method can be applied to prepare mesoporous silica with different morphologies, including sphere, fiber, nanorods, film and so on.[22-28] However, it is still difficult to control the assembly of surfactant and silica source to form mesostructure silica with various shapes in the weak acidic condition.[29-31] Furthermore, avoiding the use of strong acidic medium is highly desirable and beneficial in terms of environmental impact.[32]

Boric acid ($B(OH)_3$) is known as a weak Lewis acid (pKa = 9.237). It can interact with H_2O molecule and form the tetrahydroxyborate anion ($B(OH)_4^-$) and hydronium cation (H_3O^+).[32, 33] Previous reports have demonstrated the $B(OH)_4^-$, H_3O^+ and boric acid molecules can interact with the hydrophilic poly(ethylene oxide) moieties ($-CH_2CH_2O-$) of Pluronic P123 through polar interactions, which can promote the role of double hydrogen bonds and in favor of the assembly of mesostructures.[32, 34] These

features render boric acid highly promising in the synthesis of mesostructure materials.[35-40]

Herein, we report the utilizing of boric acid on the formation of mesostructure silica by employing the tetraethyl orthosilicate (TEOS) as precursor, commercial triblock copolymer Pluronic P123 and hexadecyltrimethylammonium bromide (CTAB) as co-surfactant. A series of mesostructure silica with various morphologies, porosities and diameters can be controllable obtained by changing the ratio of CTAB/P123, the amount of silica precursor, the addition of inorganic salt, and the concentration of boric acid and surfactant.

2. Experimental Section

2.1 Chemicals. All of chemicals were analytical grade and used without further purification. Triblock poly(ethylene oxide)-*b*-poly(propylene oxide)-*b*-poly(ethylene oxide) copolymer Pluronic P123 (PEO_{20}-PPO_{70}-PEO_{20}) was brought from Acros Corp. Hexadecyltrimethylammonium bromide (CTAB), boric acid, tetraethyl orthosilicate (TEOS), anhydrous magnesium sulfate and HCl were purchased from Sinopharm Chemical Reagent Co. (China). Ltd. Deionized water was used in all experiments.

2.2 Preparation of mesostructure silica. The mesostructure silica was synthesized via using nonionic tri-block copolymer Pluronic P123 and CTAB as the co-surfactant templates and TEOS as the silica source in the boric acid solution. As a typical synthesis of hollow silica spheres, 0.1 g of P123, 0.02 g of CTAB and 3.0 g of boric acid (1.3 mol/L) were firstly dissolved in 40 mL deionized water and stirred for 2 h. Then, 0.5 mL of TEOS was dropped into the solution with gentle stirring at 40 °C. After continuous reaction for 80 h, the solution was transferred into a 100-mL autoclave and hydrothermal treated at 100 °C for 24 h. The precipitates were collected by centrifugation and washed with deionized water several times. The P123 and CTAB surfactants were removed by calcination in atmosphere at 550 °C for 5 h to obtain the products.

2.3 Characterization. The small-angle X-ray scattering (SAXS) measurements were

taken on a Nanostar U small-angle X-ray scattering system (Bruker, Germany) using Cu Kα radiation. The *d*-spacing values were calculated by the following formula: $d = 2\pi / q$. Nitrogen sorption isotherms were measured at 77 K with a Micromeritcs Tristar 3020 analyzer (USA). Before measurements, the samples were degassed in a vacuum at 180 °C for 6 h. The Brunauer-Emmett-Teller (BET) method was utilized to calculate the specific surface areas (S_{BET}), using adsorption data in a relative pressure (P/P_0) range from 0.04 to 0.2. The pore volume and pore size distributions were derived from the adsorption branches of isotherms by using Barrett-Joyner- Halenda (BJH) model. The total pore volume, V_t, was estimated from the amount adsorbed at a relative pressure P/P_0 of 0.995. Scanning electron microscopic (SEM) images were obtained on a Philip XL30 microscope. A thin film of gold was sprayed on the samples before the characterization. Field-emission scanning electron microscopy (FESEM) images were obtained on a Hitachi S-4800 microscope (Japan). Transmission electron microscopy (TEM) measurements were achieved on a JEOL 2011 microscope operated at 200 kV. The samples were suspended in ethanol and dried on a holey carbon film on a Cu grid for TEM measurements. Fourier transform infra-red (FTIR) spectra were collected on Nicolet Fourier spectrophotometer with spectral width of 4000 – 500 cm^{-1}, using KBr pellets of the solid samples.

3. Results and Discussion

The mesostructure silica materials were synthesized by using TEOS as the silica source, nonionic tri-block copolymer Pluronic P123 and cationic CTAB as the co-surfactant templates under boric acid medium. The key to the fabrication of mesostructure silica under the weak acid condition lies in the choice of boric acid as the catalyst, which can advance the interaction between silica precursor and surfactant micelle to form mesostructures. As a typical example, hollow siliceous spheres can be simply prepared by using P123 (0.1 g) and CTAB (0.02 g) as co-surfactant templates and TEOS (0.5 mL) as the silica source in boric acid solution (1.3 mol/L). The

small-angle X-ray scattering (SAXS) pattern of the obtained product (denoted as S1) displays an obvious wide peak at q = 0.07 (Fig. 1A-S1), indicating a certain extent of ordered mesostructure. The scanning electron microscopic (SEM) image reveals the sample S1 composing with tiny nanoparticles (Fig. S1A). As confirmed by field-emission scanning electron microscopy (FESEM) image, spherical mesostructure silica nanoparticles were synthesized with a size of ~ 15 nm (Fig. 1B), similar to that single spherical micelles spheres. Transmission electron microscopy (TEM) image clearly shows the spherical mesostructure silica nanoparticles exhibited a remarkable hollow structure with the cavity of ~ 7 nm and a thin silica shell of ~ 2 nm in thickness (Fig. 1B, inset). N_2 sorption isotherms of the hollow siliceous spheres (Fig. 2A-S1) present a typical type-IV curve consisting with a distinct H1-type hysteresis loop in the broad relative pressure (p/p_0) range of 0.4 - 0.9, indicating the presence of mesopores. Furthermore, the adsorption branch exhibits two capillary condensation steps at high relative pressure (p/p_0) of 0.5 - 0.7 and 0.8 - 0.95, respectively, suggesting the formation of large and multimodal pore size distribution. Corresponding, the pore size distribution calculated by using Barrett-Joyner- Halenda (BJH) model with adsorption branch (Fig. 2B-S1), shows a bimodal pore size distribution centered at 6.7 and 35 nm, respectively, originated from the cavity diameter and accumulation of the hollow spheres. This phenomenon is good agreement with the TEM result (Fig. 1B, inset). Moreover, the hollow siliceous spheres possess a large pore volume of 1.82 cm^3g^{-1} and the high Brunauer-Emmett-Teller (BET) surface area of 515.0 m^2g^{-1} (Table 1).

Similarly, a series of mesostructure silica materials with various morphologies and porosities have been successfully prepared using P123 and CTAB as the co-surfactant templates, and TEOS as the silica source in boric acid solution. The detailed experimental conditions and corresponding surface areas, pore sizes and pore volumes are summarized in Table 1. It is noteworthy that the morphologies, porosities and diameters of the mesostructure silica materials are highly dependent on the ratio of CTAB/P123, the concentration of boric acid, the amount of silica precursor, the addition of inorganic salt, and the concentration of surfactant.

The ratio of CTAB/P123 has been considered to investigate the morphology and porosity. As the relative proportion of CTAB increase from 0.04 to 0.06 g (S2 and S3), the scattering peak becomes poorly resolved (Fig. 1A-S2 and -S3). Further increasing the CTAB amount to 0.1 g without the addition of P123 (S4), a clear broad peak appears at q value of ~ 0.13 $Å^{-1}$, suggesting only using CTAB as a surfactant also can form the ordered mesostructure silica (Fig. 1A-S4). According, with the P123 as the single surfactant (0.1g, S5), two distinguished scattering peaks indexes as 10 and 20 reflection can be observed associating with the *p6mm* hexagonal structure (Fig. 1A-S5). The sample S2, S3 and S4 show spherical particle shape with very small size (Fig. S1B-D and Fig. 1C-E). TEM images reveal the nanoparticles are hollow siliceous spheres with the shell thickness of ~ 2 nm and cavity diameter about 7, 7 and 2 nm, respectively (Fig. 1C-E, inset). The oligomeric tubular silica is also can be produced, as shown by the SEM, FESEM and TEM images (Fig. S1E and Fig. 1F), with the inner diameter of ~ 10 nm, wall thickness of ~ 2 nm and the length of ~ 200 nm. Nitrogen sorption isotherms of these samples are shown in Fig. 2. All the isotherms of the samples (S2 - S5) are type-IV curves accompanying with the prominent hysteresis in a broad relative pressure (p/p_0) range from 0.4 to 0.9. The BET surface areas for the mesostructure silica samples S2 to S5 are in the range of 330.0 to 716.6 m^2g^{-1}, the pore volumes changed from 1.00 to 2.07 cm^3g^{-1}, and pore sizes varied from 2.2 to 9.2 nm as listed in Table 1. These results indicate that the ratio of CTAB/P123 indeed can affect the morphologies and porosities of mesostructure silica materials.

To confirm the role of boric acid in the formation of mesostructure silica, other concentrations of boric acid, 0.32 and 2.5 mol/L (S6 and S7) were selected to further examine the physicochemical properties. It can be found that the spherical mesostructure silica nanoparticles still are obtained at such low and high concentrations (Fig. 3 A and 3B). Furthermore, this mesostructure silica nanopaticles display ordered mesostructure in some extent, as revealed by the broad scattering peaks in the SAXS pattern (Fig. S2). What is more, the sample S6 and S7 exhibit the type-IV isotherms and bimodal pore size distribution (Fig. 3C and 3D), close to that

of sample S1 with the concentration of boric acid of 1.3 mol/L. Especially, the surface area (500.0 and 595.1 m^2g^{-1}), pore volume (1.89 cm^3g^{-1}) and pore size (7.4 and 6.5 nm) of sample S6 and S7 are nearly the same for the sample S1 (Table 1), suggesting the concentration of boric acid has little effect on the morphology and porosity. Interestingly, the mesostructure silica can not be prepared if the boric acid is replaced with other weak acid at the same reaction condition, such as acetic acid at the pH of ~3 (Fig. S3). This further verifies the vital role of boric acid in the formation of mesostructure silica.

It was also found that the amount of silica precursor plays a significant impact in the morphology. With the addition amount of TEOS decrease from 0.5 to 0.25 mL (S8), uniform tubular mesostructure silica is obtained with the width of ~ 15 nm and several hundred nanometers in length (Fig. 4A). The tubular mesostructure silica presents a broad scattering peak in SAXS pattern and the type-IV isotherms with a H1-type hysteresis loop (Fig. S4), demonstrating the tubular ordered mesostructure. The inner diameter can be calculated to be ~ 11.8 nm from the adsorption branch by using the BJH modal. The formation of tubular mesostructure silica with large hollow inner and thin thickness is ascribed to the lower concentration of silica source, reducing the curvature of the micelles and optimizing the assembly between surfactant and silica precursor.

With the addition of $MgSO_4$, the obtained mesostructure silica (S9) shows a well-resolved scattering peak (Fig. S5). It reveals that $MgSO_4$ additive facilitates the assembly of CTAB/P123 co-surfactant and silica source due to the enhanced interactions, and improves the ordering of mesostructure. This speculation can be confirmed by the phenomena that the hollow siliceous spheres are inclined to aggregate together (Fig. 5A and 5B), combined with the decreasing of surface area (304.2 m^2g^{-1}), pore volume (0.93 cm^3g^{-1}) and uniform pore size distribution (6.0 nm) (Fig. 5C and 5D and Table 1).

To explore the influence of concentration of surfactant, three additional high concentrations of surfactant (S10: 1.0 g P123 + 0.2 g CTAB; S11: 1 g CTAB; and S12: 1g P123) conditions were taken into account. SAXS pattern of the samples shows one

wide peak (Fig. S6), indicating the formation of not highly ordered mesostructure. The morphologies of sample S10 and S11 still unchange with the composed of small hollow siliceous spheres (Fig. 6A and 6B). However, it should be noted that the cage-like mesostructure silica with the size of ~ 1 μm can be synthesized (S12, Fig. 6C). The structure of the cage-like mesostructure is similar in profile of human brain, binding with ~ 50 nm diameter bundles. TEM image shows the congregating together of bundles consisting of 3 - 4 layers of tubular silica (Fig. 6D and inset). Moreover, N_2 sorption isotherms of these mesostructure silica samples (S10, S11 and S12) exhibit typical type IV curves with a H2-type hysteresis loop (Fig. S7). However, the pore volume and pore size undergo a little decreasing with the increasing of BET surface area (Table 1).

Considering the facts of the prepared of mesostructure silica materials. Here, the key point of the formation of mesostructure silica with various morphologies and porosities are highly dependent on the boric acid assisted assembly of CTAB and P123 co-surfactant with silica source. It is worth noting that the $B(OH)_3$ can reacted with H_2O molecule to result the formation of $B(OH)_4^-$ anion and H_3O^+ cation.[32, 33] Simultaneously, the H_3O^+ and boric acid oligomer ($B(OH)_4^-$ and boric acid molecules) associate with the hydrophilic poly(ethylene oxide) moieties ($-CH_2CH_2O-$) of Pluronic P123 through polar interactions, hydrogen bond and van der Waals forces, which can promote the role of double hydrogen bonds and advance the assembly of surfactants and inorganic species. As a consequence, the silicate species originate from the hydrolysis and condensation of TEOS precursor can combine with H_3O^+ and CTA^+ through electrostatic interaction to construct the micelles assembly at such ultra-dilute CTAB/P123 surfactant condition and different concentrations of boric acid (Fig. 7).[32, 34] Furthermore, the boric acid also can directly link with Si-OH to form the B-O-Si bond, which is easily hydrolyzes. This not stable B-O-Si bond results the B species can be easily removed after the hydrothermal and post-treatment process, which can be verified by the undetectable characteristic bands of boric acid (550, 884 and 1192 cm^{-1}) and the peak of B-O-Si (910 cm^{-1}) for mesostructure silica materials in the FTIR spectra (Fig. S8).[33, 34, 36] On the other hand, the CTAB surfactant is prone to

formation of spherical micelles and results the synthesis of hollow siliceous spheres (S1 - S4).[41] The spherical micelles behaviors are inclined to transform to tubular micelles with the decreasing of silica source (S8) or without the addition of CTAB surfactant (S5). Particularly, the addition of $MgSO_4$ can promote the interaction of inorganic and organic species and regular mesostructure (S9). Furthermore, the higher concentration of surfactant is advantage for the assembly to hierarchical mesostructure (S10 - S12).

4. Conclusion

In conclusion, the boric acid assisted assembly approach has been successfully demonstrated to synthesize the mesostructure silica with controllable morphologies and porosities. A series of mesostructure silica such as hollow siliceous spheres, tubular and cage-like mesoporous silica were prepared by using CTAB/P123 as co-surfactant, TEOS as the silica source in the boric acid medium. The ratio of CTAB/P123, the concentration of boric acid and surfactant, the amount of TEOS and the addition of $MgSO_4$ were all considered to evaluate the physicochemical properties of the mesostructure silica. It reveals the obtained mesostructure silica materials possess uniform morphologies, high surface area (304.2 – 742.0 m^2g^{-1}), tunable large pore volume (0.55 – 2.07 cm^3g^{-1}) and pore size distribution (2.2 – 11.8 nm). Importantly, this boric acid assisted approach is facile and reproducible under weak acid condition. It is believed that this boric acid assisted strategy can be applied to synthesize other mesostructure materials. Moreover, the obtained hollow spheres and tubular mesoporous silica can serve as the good candidates for catalyst and bioapplications.

Acknowledgements

The work was supported by NSFC Grant 21277102 and Science and Technology Commission of Shanghai (Grant 11JC1412600).

References

1. Y. Ren, Z. Ma and P. G. Bruce, *Chem. Soc. Rev.*, 2012, **41**, 4909-4927.
2. W. Li, Q. Yue, Y. H. Deng and D. Y. Zhao, *Adv. Mater.*, 2013, **25**, 5129-5152.
3. Y. Yamauchi and K. Kuroda, *Chem. –Asian J.*, 2008, **3**, 664-676.
4. A. Corma, *Chem. Rev.*, 1997, **97**, 2373-2420.
5. A. Taguchi and F. Schüth, *Microporous Mesoporous Mater.*, 2005, **77**, 1-45.
6. Z. X. Wu and D. Y. Zhao, *Chem. Commun.*, 2011, **47**, 3332-3338.
7. A. Walcarius, *Chem. Soc. Rev.*, 2013, **42**, 4098-4140.
8. Z. X. Li, J. C. Barnes, A. Bosoy, J. F. Stoddart and J. I. Zink, *Chem. Soc. Rev.*, 2012, **41**, 2590-2605.
9. Y. Wan and D. Y. Zhao, *Chem. Rev.*, 2007, **107**, 2821-2860.
10. Y. Wan, Y. F. Shi and D. Y. Zhao, *Chem. Commun.*, 2007, 897-926.
11. H.-P. Lin and C.-Y. Mou, *Acc. Chem. Res.*, 2002, **35**, 927-935.
12. A. H. Lu and F. Schüth, *Adv. Mate.*, 2006, **18**, 1793-1805.
13. B. G. Trewyn, I. I. Slowing, S. Giri, H.-T. Chen and V. S. Y. Lin, *Acc. Chem. Res.*, 2007, **40**, 846-853.
14. D. Tarn, C. E. Ashley, M. Xue, E. C. Carnes, J. I. Zink and C. J. Brinker, *Acc. Chem. Res.*, 2013, **46**, 792-801.
15. F. Q. Tang, L. L. Li and D. Chen, *Adv. Mater.*, 2012, **24**, 1504-1534.
16. J. L. Vivero-Escoto, I. I. Slowing, B. G. Trewyn and V. S. Y. Lin, *Small*, 2010, **6**, 1952-1967.
17. J. P. Yang, D. K. Shen, L. Zhou, W. Li, J. W. Fan, A. M. El-Toni, W. -x. Zhang, F. Zhang and D. Y. Zhao, *Adv. Healthcare Mater.*, 2014, DOI: 10.1002/adhm.201400053.
18. L. M. Pan, Q. J. He, J. N. Liu, Y. Chen, M. Ma, L. L. Zhang and J. L. Shi, *J. Am. Chem. Soc.*, 2012, **134**, 5722-5725.
19. J. P. Yang, D. K. Shen, L. Zhou, W. Li, X. M. Li, C. Yao, R. Wang, A. M. El-Toni, F. Zhang and D. Y. Zhao, *Chem. Mater.*, 2013, **25**, 3030-3037.
20. D. K. Shen, J. P. Yang, X. M. Li, L. Zhou, R. Y. Zhang, W. Li, L. Chen, R. Wang, F. Zhang and D. Y. Zhao, *Nano Lett.*, 2014, **14**, 923-932.
21. D. Y. Zhao, J. L. Feng, Q. S. Huo, N. Melosh, G. H. Fredrickson, B. F. Chmelka and G. D. Stucky, *Science*, 1998, **279**, 548-552.
22. H. Yang, N. Coombs and G. A. Ozin, *Nature*, 1997, **386**, 692-695.
23. D. Y. Zhao, J. Y. Sun, Q. Z. Li and G. D. Stucky, *Chem. Mater.*, 2000, **12**, 275-279.
24. K. Kosuge, T. Sato, N. Kikukawa and M. Takemori, *Chem. Mater.*, 2004, **16**, 899-905.
25. W. J. J. Stevens, K. Lebeau, M. Mertens, G. Van Tendeloo, P. Cool and E. F. Vansant, *J. Phys. Chem. B*, 2006, **110**, 9183-9187.
26. P. Linton and V. Alfredsson, *Chem.Mater.*, 2008, **20**, 2878-2880.
27. S.-Y. Chen, C.-Y. Tang, W.-T. Chuang, J.-J. Lee, Y.-L. Tsai, J. C. C. Chan, C.-Y. Lin, Y.-C. Liu and S. Cheng, *Chem. Mater.*, 2008, **20**, 3906-3916.
28. C. Z. Yu, J. Fan, B. Z. Tian and D. Y. Zhao, *Chem. Mater.*, 2004, **16**, 889-898.
29. J. T. Tang, J. Liu, P. Y. Wang, H. Zhong and Q. H. Yang, *Microporous*

Mesoporous Mater., 2010, **127**, 119-125.
30. O. Aktas, S. Yasyerli, G. Dogu and T. Dogu, *Mater. Chem. Phys.*, 2011, **131**, 151-159.
31. H. N. Wang, Y. H. Wang, X. F. Zhou, L. Zhou, J. W. Tang, J. Lei and C. Z. Yu, *Adv. Funct. Mater.*, 2007, **17**, 613-617.
32. S. L. Ding, N. Liu, X. W. Li, L. M. Peng, X. F. Guo and W. P. Ding, *Langmuir*, 2010, **26**, 4572-4575.
33. E.-B. Cho, M. Mandal and M. Jaroniec, *Chem. Mater.*, 2011, **23**, 1971-1976.
34. J. P. Yang, F. Zhang, W. Li, D. Gu, D. K. Shen, J. W. Fan, W.-x. Zhang and D. Y. Zhao, *Chem. Commun.*, 2014, **50**, 713-715.
35. D.-W. Wang, F. Li, Z.-G. Chen, G. Q. Lu and H.-M. Cheng, *Chem.Mater.*, 2008, **20**, 7195-7200.
36. H. I. Lee, G. D. Stucky, J. H. Kim, C. Pak, H. Chang and J. M. Kim, *Adv. Mater.*, 2011, **23**, 2357-2361.
37. N. Wickramaratne and M. Jaroniec, *Rsc Adv.*, 2012, **2**, 1877-1883.
38. C. Moreno-Castilla, M. B. Dawidziuk, F. Carrasco-Marín and Z. Zapata-Benabithe, *Carbon*, 2011, **49**, 3808-3819.
39. J. C. Zhang, M. Liu, C. S. Song and X. W. Guo, *Microporous Mesoporous Mater*, 2011, **139**, 31-37.
40. S. L. Ding, S. J. Zheng, M. J. Xie, L. M. Peng, X. F. Guo and W. P. Ding, *Microporous Mesoporous Mater.*, 2011, **142**, 609-613.
41. J. P. Yang, F. Zhang, Y. R. Chen, S. Qian, P. Hu, W. Li, Y. H. Deng, Y. Fang, L. Han, M. Luqman and D. Y. Zhao, *Chem. Commun.*, 2011, **47**, 11618-11620.

Table 1. Physicochemical properties of mesostructure silica prepared by using nonionic tri-block copolymer Pluronic P123 and CTAB as the co-surfactant templates and TEOS as the silica precursor in the boric acid solution.

Sample	Boric acid (mol/L)	P123 (g)	CTAB (g)	$MgSO_4$ (g)	TEOS (mL)	S_{BET} (m^2/g)	Vt (cm^3/g)	Pore size [a] （nm）
S1	1.3	0.1	0.02	/	0.5	515.0	1.82	6.7
S2	1.3	0.1	0.04	/	0.5	532.2	2.07	6.7
S3	1.3	0.1	0.06	/	0.5	496.8	2.01	7.4
S4	1.3	/	0.1	/	0.5	330.0	1.00	2.2, 22.6
S5	1.3	0.1	/	/	0.5	716.6	1.72	9.2
S6	0.32	0.1	0.02	/	0.5	500.0	1.89	7.4, 40
S7	2.5	0.1	0.02	/	0.5	595.1	1.89	6.5, 31
S8	1.3	0.1	0.02	/	0.25	502.8	1.13	11.8
S9	1.3	0.1	0.02	0.35	0.5	304.2	0.93	6.0
S10	1.3	1	0.2	/	2.5	620.1	0.76	4.6
S11	1.3	/	1	/	2.5	705.8	0.70	5.6
S12	1.3	1	/	/	2.5	742.0	0.55	5.4

[a] pore size distributions were derived from the adsorption branches of isotherms by using Barrett-Joyner- Halenda (BJH) model.

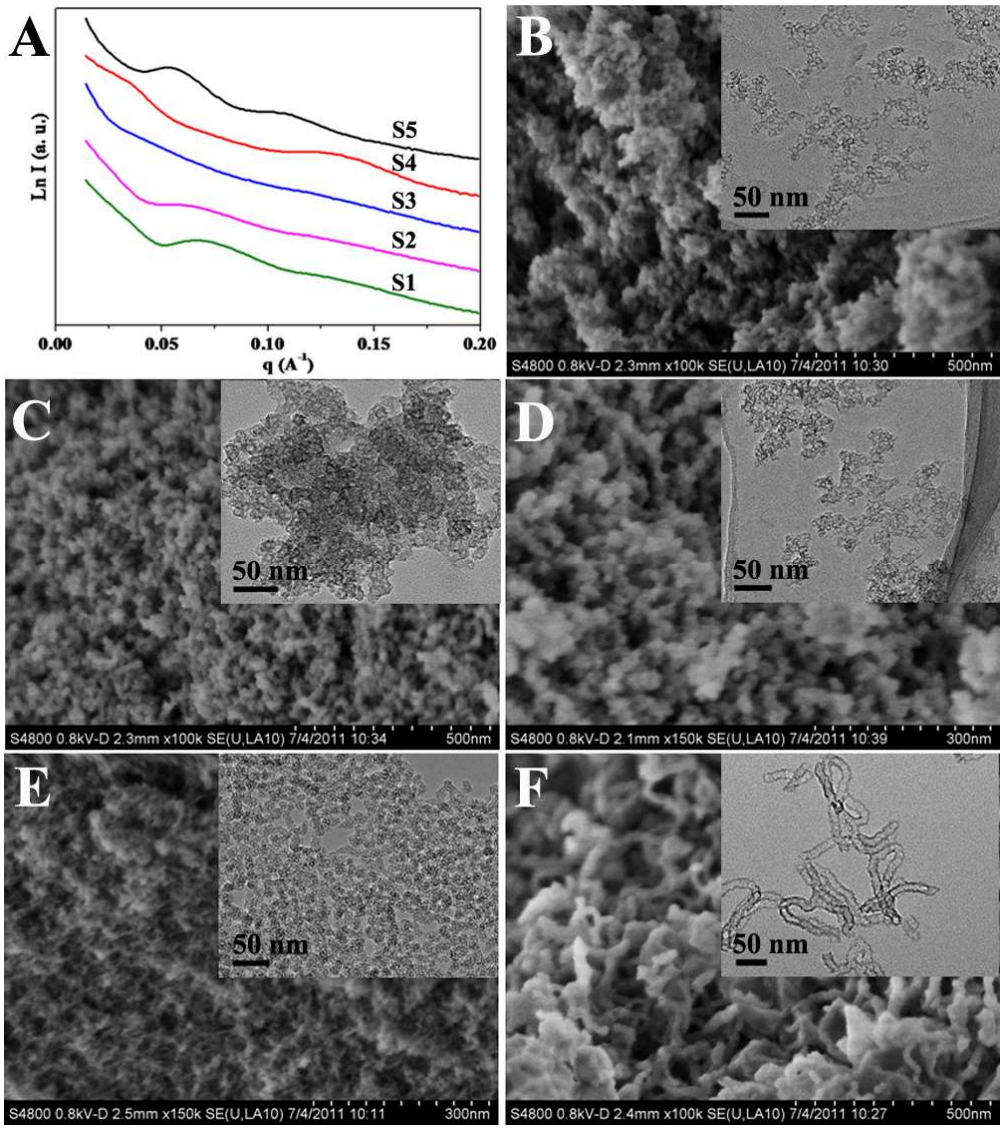

Fig. 1 SAXS pattern (A) and FESEM images of mesostructure silica: (B) S1, (C) S2, (D) S3, (E) S4 and (F) S5. Insets show the corresponding TEM images. The mesoporous silica hollow spheres and nanotubes (S1 to S5) are prepared by using different CTAB amount (0.02, 0.04, 0.06, 0.1 and 0 g) and P123 (0.1 g) as template and TEOS (0.5 mL) as the silica precursor in boric acid solution (1.3 mol/L).

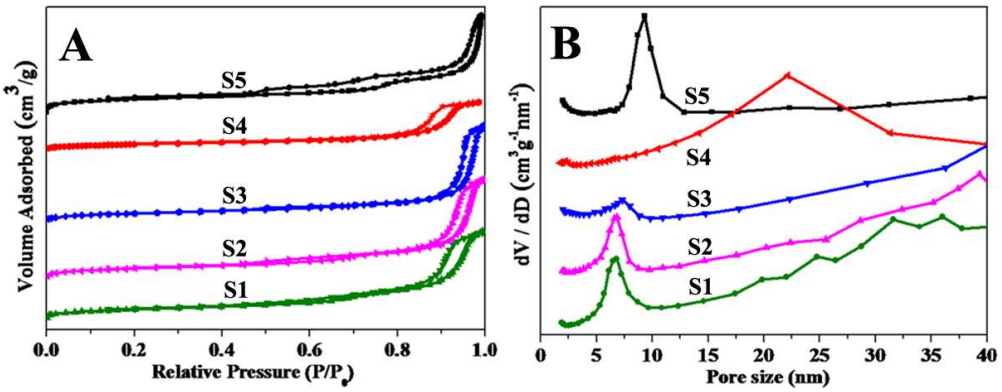

Fig. 2 N_2 sorption isotherm curves (A) and pore size distribution plots (B) of mesostructure silica S1, S2, S3, S4 and S5. Isotherm and pore size distribution curves are shifted for clarity. The mesostructure silica (S1 to S5) are prepared by using different CTAB amount (0.02, 0.04, 0.06, 0.1 and 0 g) and P123 (0.1 g) as template and TEOS (0.5 mL) as the silica precursor in boric acid solution (1.3 mol/L).

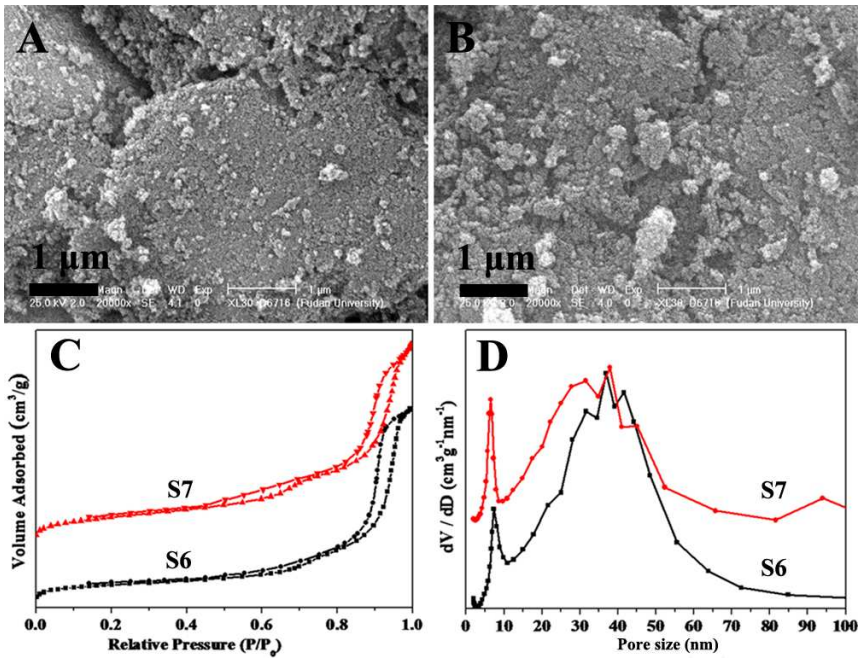

Fig. 3 SEM images of (A) S6 and (B) S7, N_2 sorption isotherm curves (C) and pore size distribution plots (D) of mesostructure silica S6 and S7. Isotherm and pore size distribution curves are shifted for clarity. The mesostructure silica (S6 and S7) are prepared by using CTAB (0.02 g) and P123 (0.1 g) as template andTEOS (0.5 mL) as the silica precursor in different concentration of boric acid solution (0.32 and 2.5 mol/L).

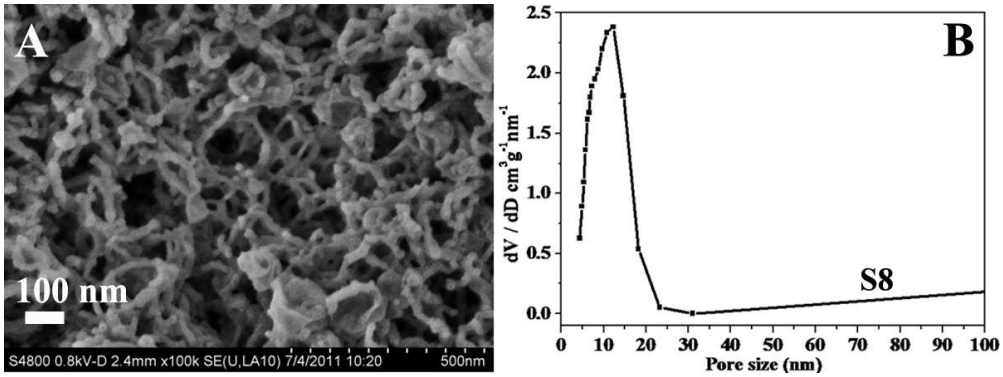

Fig. 4 FESEM image (A) and pore size distribution plot (B) of mesostructure silica S8. The mesostructure silica S8 sample is prepared by using CTAB (0.02 g) and P123 (0.1 g) as template and low volume of TEOS (0.25 mL) as the silica precursor in boric acid solution (1.3 mol/L).

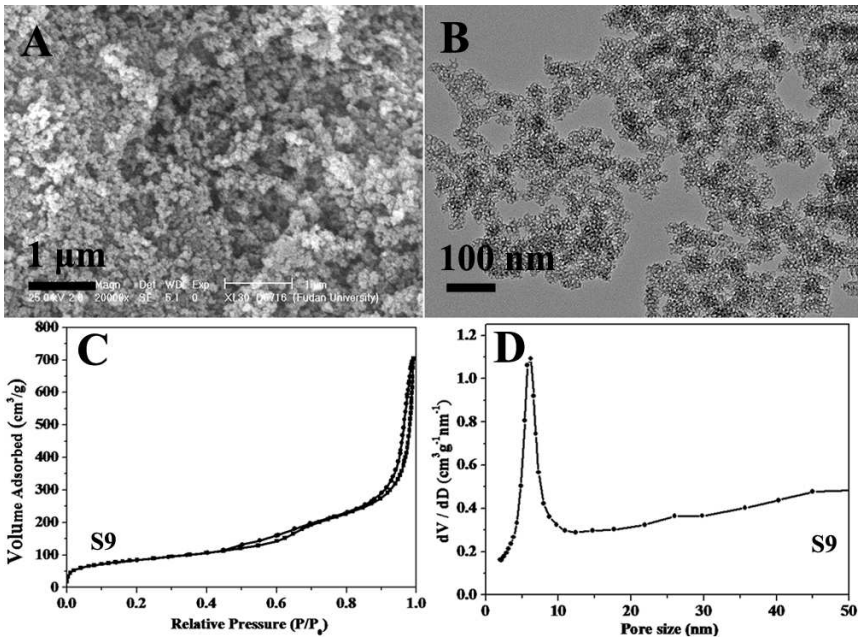

Fig. 5 Typical SEM (A), TEM images (B), N_2 sorption isotherm curves (C) and pore size distribution plot (D) of mesostructure silica S9. The mesostructure silica S9 sample is prepared by using CTAB (0.02 g) and P123 (0.1 g) as template, TEOS (0.5 mL) as the silica precursor and $MgSO_4$ (0.35 g) as the inorganic salt in boric acid solution (1.3 mol/L).

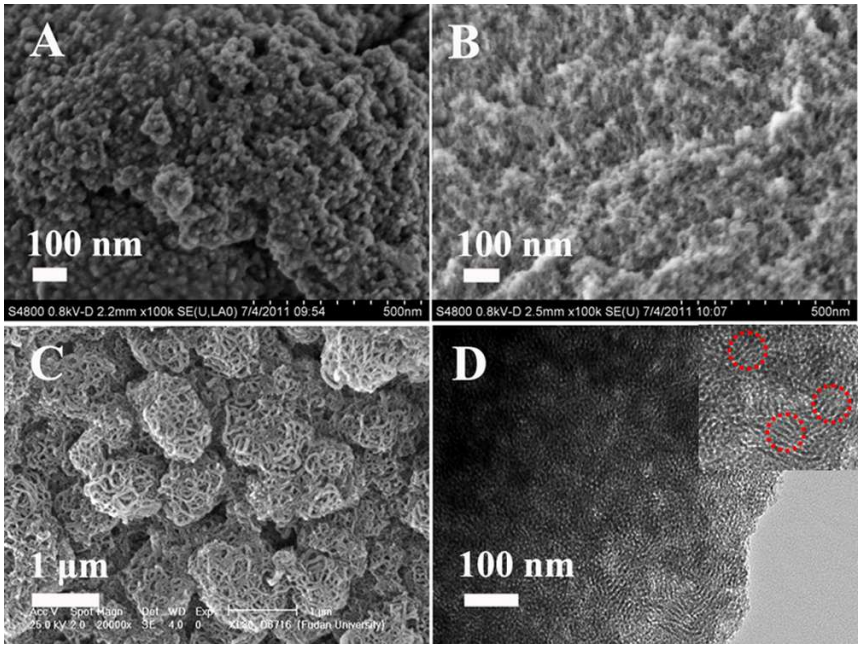

Fig. 6 FESEM images of mesostructure silica: (A) S10 and (B) S11, SEM (C) and TEM (D) images of mesostructure silica S12. The mesostructure silica samples (S10, S11 and S12) are prepared by using high concentration of surfactants: CTAB (0.2, 1.0 and 0 g) and P123 (1.0, 0 and 1 g), and TEOS (2.5 mL) as the silica precursor in boric acid solution (1.3 mol/L).

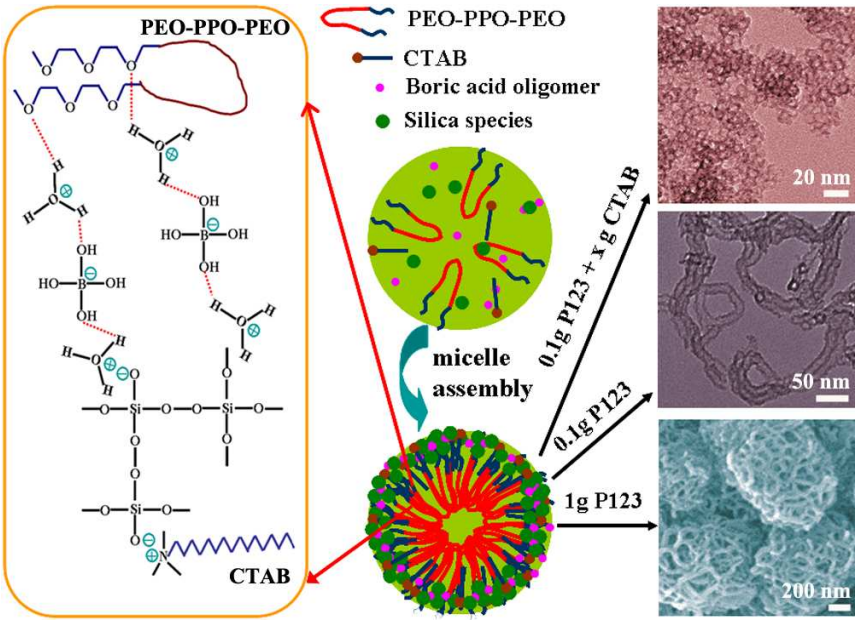

Fig. 7 Schematic illustration of the formation of mesostructure silica materials through boric acid assisted assembly approach by using CTAB/P123 as co-surfactant and TEOS as the silica source.

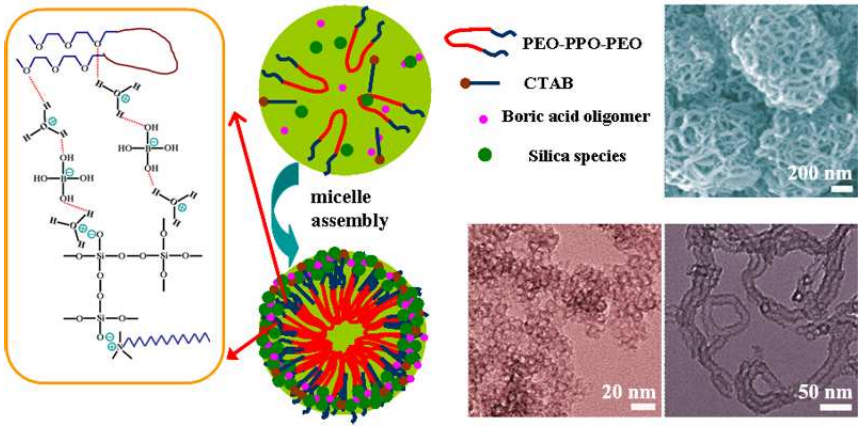

A boric acid assisted assembly approach has been provided to prepare the mesostructure silica with various morphologies and porosities.